



Quaternary Functionalized Cellulose-based Biopolymer for Anion Exchange Membrane Fabrication

U.F. Kandil^{1*}, E.O. Taha¹, E.A. Mahmoud¹, M. Mahmoud², M.M. Reda Taha³

¹ Petroleum Applications Department, Egyptian Petroleum Research Institute, Nasr City 11727,

Cairo, Egypt.

² Water Pollution Research Department, National Research Centre, Dokki, Cairo 12311, Egypt.

³ Department of Civil, Construction & Environmental Engineering, University of New Mexico, Albuquerque, NM 87131-0001, USA.



CrossMark

Abstract

In this work, we introduce a new method for preparing an enhanced anion exchange membrane (AEM) based on biopolymer (cellulose) for water treatment. The preparation and fabrication of AEM were performed by chlorinating cellulose powder to prepare chlorodeoxycellulose (CDC) and then quaternizing CDC with dimethyl amine to prepare quaternized dimethylamine cellulose (QDC). The quaternized polymeric material was used to fabricate the exchange membrane. Membrane porosity was controlled by incorporating polyethylene glycol as a pore former with different ratios using the phase inversion technique. The performance of the fabricated AEM was fully investigated by studying the relationship between the pore former content and the pore characteristics, including porosity, water uptake, swelling ratio, and ion exchange capacity. The microstructure and morphology of the membrane were also examined and discussed.

Keywords: anion exchange membrane, pore former, quaternization

1. Introduction

Clean fresh drinking water is an essential element of human life. Despite the fact that water is an abundant natural resource, 97% of the Earth's water is seawater; it cannot be used directly for drinking without additional treatment [1]. Furthermore, although the remaining 3% is freshwater, only 1% of it is available for direct use. The accessibility of freshwater is a key challenge for economic development in many countries. Water desalination technologies can provide a viable solution to meet the demand for freshwater supply [2]. The shortage of clean freshwater derived several research attentions towards desalination methods using different membrane technologies such as nanofiltration and reverse osmosis that have recently become the most common methods for water desalination [3].

Ion exchange membranes (IEM) have undergone extensive research activities in the last century [4]. The membrane separation procedure is one of the most promising technologies for water desalination.

Membrane technology is an effective and economical means owing to its low energy consumption, easy set-up, and limited usage of chemicals. Furthermore, membrane technology does not create any hazardous by-products [5]. It is well known that an ion-exchange membrane is a semi-permeable membrane that transports certain dissolved ions while blocking other ions or neutral molecules [6]. Therefore, ion-exchange membranes are often used in water desalination and chemical recovery applications, moving ions from one solution to another [7]. El-Gohary et al., used membrane bioreactor technology for wastewater reclamation, where they achieved efficient removals of suspended solids, organic contaminants, parasites, and fecal coliform bacteria [8]. Abd Elnasser et al., produced a silver ion-selective membrane based on a newly synthesized compound derived from the reaction of 2-acetyl thiophene with 2-aminophenol [9]. Abdel-Shafy et al., showed the efficiency of bio-membranes for water and wastewater treatment. They claimed that

*Corresponding author e-mail: alfa_olefins@yahoo.com.

Receive Date: 14 October 2021, Revise Date: 14 November 2021, Accept Date: 23 February 2022

DOI: 10.21608/EJCHEM.2022.101109.4698

©2022 National Information and Documentation Center (NIDOC)

cleaned water production could be achieved without any hazardous pollutants, and the treated wastewater can be reused safely for non-potable purposes such as irrigation or flushing [10].

Recently, functionalization of some polymers has been performed to form quaternary ammonium moieties for manufacturing AFMs [11]. This functionalization has been performed by halogenation followed by quaternization of polymers such as polysulfone [12,13], PPO [14,15], poly(phenylene) [16], and poly(arylene ether ketone) [17]. Orlando et al., converted natural waste materials into anion-exchangers through functionalization. They produced weak-base anion-exchangers with tertiary amines as major functional exchange groups from WNM and mixtures of pure lignin and pure cellulose [18]. Careful selection of the polymeric materials to be used in membrane fabrication might be necessary such that the material can resist stresses applied to the membrane during service [19]. The ion-selective membrane has become an outstanding technology for several applications. Producing specific ion exchangers is widely used in water desalination and wastewater treatment plants.

This work introduces the use of functionalized matrix membranes consisting of cellulose as a polymer and polyethylene glycol (PEG) as a pore former with different contents. The mixture is used to produce an enhanced anion exchange membrane (AEM). Cellulose was firstly functionalized, followed by membrane fabrication with the aid of PEG. The fabricated AFM was fully investigated, including studying its microstructure and morphology. In addition, the relationship between the pore former content and the pore characteristics, including; porosity, water uptake, swelling ratio, and ion exchange capacity, were investigated and discussed.

2. Experimental Methods

The goal of this work was to synthesize specific functional polymeric material to be suitable for the fabrication of anion exchange membranes. In this work, cellulose was firstly chlorinated with thionyl chloride to produce chlorodeoxycellulose (CDC). The chlorination process is favored by nucleophilic thionyl chloride attack on the hydroxyl group in the cellulose backbone, resulting in pendant chlorine atoms on the polymeric structure, as shown in **Figure 1** [20].

This substituted atom is much more reactive than the original hydroxyl group, and consequently, it was used for the quaternization step using dimethylamine to prepare quaternized dimethylamine cellulose (QDC) [21]. Finally, QDC was treated with

potassium hydroxide to afford the polymeric material suitable for anion exchange membrane fabrication [22].

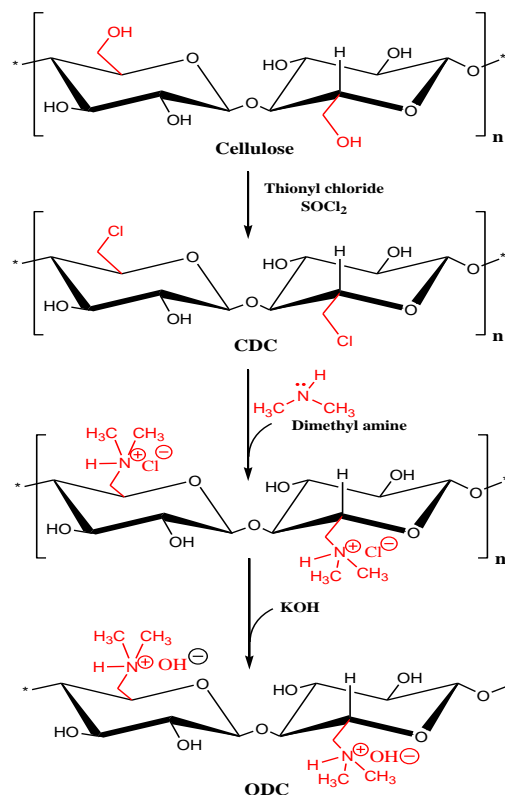


Figure 1: Schematic diagram for the synthesis of QDC membrane [20].

Materials

Microcrystalline cellulose as a powder (Sigma Aldrich), ~ 20 μm, was dried before use. Polyethylene glycol (PEG, MWt, 600), dimethylamine, N,N'-dimethylformamide (DMF) and thionyl chloride (SOCl₂) were purchased from Sigma Aldrich. HCl, NaOH, KOH, and acetone were all reagent grade and used without prior purification.

Synthesis of chlorodeoxycellulose (CDC)

10 g of cellulose powder was suspended in 200 ml N,N-dimethylformamide (DMF) in a round-bottomed flask equipped with a reflux condenser at 80°C for 1 hour. Then, 35 ml of thionyl chloride was drop-wisely added under vigorous stirring. Because the reaction is exothermic, the addition speed was carefully controlled so that the temperature was kept between 95 and 100°C. After the addition was completed, the stirring was continued for 2 hours at the same temperature. The resulting mixture was washed with acetone and deionized water and finally was dried in a vacuum at room temperature [23,24].

Synthesis of quaternized dimethylamine cellulose (QDC)

10 g of CDC was reacted with 100 ml of 50% dimethylamine solution at 90 °C and stirred continuously for 3 hours to introduce amine functional groups. The final product was filtered and washed with 0.1 M HCl, and finally converted to hydroxide anion by washing with 0.1 M NaOH solution. The product was dried at 40 °C for 4 hours [25].

Preparation of Anion Exchange Membrane

The prepared functionalized QDC was used to fabricate the anion exchange membrane. The fabrication process was performed via the phase separation technique using polyethylene glycol (PEG, MWt, 600) [26,27]. In this method, QDC was dissolved in acetone in an amount of 20 wt. %, then PEG was added to the cellulose solution as pore former at different content (2, 5, 10, 15, and 20wt.% by weight of the cellulose), keeping the total polymer at 20wt.%. The polymeric solution mixture was ultrasonically homogenized for 30 minutes, followed by casting on a glass plate using a casting knife with a thickness of 250 µm. The glass plate with the casted solution was immediately immersed in water for creating instantaneous phase inversion between solvent and water in the coagulation bath [28]. The membrane was then separated from the glass plate, rinsed with freshwater, and then dried at 60°C. In the last step of preparation, the QDC membrane was soaked in an aqueous solution of 1M KOH for 48 h to alkalinize the $\{N^+(CH_3)_3Cl^-\}$ groups into $\{N^+(CH_3)_3OH^-\}$ groups. Then, the alkalinized QDC membrane was washed with deionized water and soaked in deionized water with frequent water changes for at least 48 hours to remove the trapped KOH [29].

Membrane characterization

Porosity, water uptake, swelling ratio, and ion-exchange capacity

QDC membranes with dimensions of (Length X Wide X Thickness = 50 mm X10 mm X 100µm thickness) were fabricated and immersed in deionized water at room temperature for 24 hours. QDC membranes were then taken out to remove the surface water by wiping with a clean tissue and weighed immediately. This was followed by drying the membranes under vacuum at 60°C until obtaining constant weight.

The porosity characteristics of the QDC membranes were assessed according to their dry-wet weight procedure as reported in the literature [30,31,32]. The weight of the QDC membrane in the wet state was recorded after eliminating the excess water. These membranes were dried in an oven at about 80 °C for

24 h, and the dry weight was recorded. The porosity of the membranes was assessed as follows:

$$\varepsilon(\%) = \frac{W_2 - W_1}{DAH} \times 100\% \dots \dots \dots 1$$

Where ε is the membrane porosity, D is the water density (0.998 g/cm³), A is the area of the membrane in cm², and H is the thickness of the membranes in cm. The weight and thickness of the samples before and after the treatments were recorded. The average water uptake (WU) of three samples was calculated using Equation (2) [33].

$$WU(\text{wt.}\%) =$$

$$\frac{W_2 - W_1}{W_1} \times 100\% \dots \dots \dots 2$$

where W_1 and W_2 are the dry and wet weights of the sample, respectively. The average value of the swelling ratio was calculated from three samples by evaluating the change in the film thickness using Equation (3).

$$SR(\%) = \frac{H_2 - H_1}{H_1} \times 100\% \dots \dots \dots 3$$

Where H_1 and H_2 are the thicknesses of the dry and wet membrane samples, respectively.

The ion-exchange capacities (IECs) of QDC membranes were determined by the back-titration method [34,35]. In this method, three dried pieces of the measured membrane (about 100 mg) were accurately weighed and then immersed in 25mL of 0.05 M hydrochloric acid (HCl) solution for 48 hours. Then, the HCl solution was back-titrated by a standardized KOH solution (0.05 M) using phenolphthalein as the indicator. The IEC values of the samples were calculated from the titration results using Equation (4).

$$IEC(\text{mmol/g}) = \frac{N_1 - N_2}{M_{dry}} \times 100\% \dots \dots \dots 4$$

where N_1 and N_2 are the amounts of HCl in mmol required before and after equilibrium, respectively. M_{dry} is the weight in (g) of the dried membrane sample. The average value of the IEC of three samples was calculated.

Fourier Transform Infrared Spectroscopy

The microstructural analysis of the prepared membranes has been performed using attenuated total reflection Fourier Transform Infrared spectroscopy (ATR-FTIR, Alpha Bruker Platinum, 1-211-6353), using a zinc selenide crystal with an incident angle of $45 \pm 15^\circ$ and 560 scan time (24 s) at 4 cm⁻¹ resolution. The spectral range used for FTIR was 500 – 4000 cm⁻¹.

Thermal Stability of QDC

Thermal gravimetric analysis (TGA) was performed to analyze the thermal properties of QDC and the microcrystalline cellulose using a thermogravimetric analyzer (TGA 55, TA) at a heating rate of 10 °C/min over a temperature range from the ambient environment to 600 °C under a nitrogen atmosphere.

The degree of substitution (DS %) in QDC was calculated based on **Figure 3** using Equation (5) [36]

$$DS \% = \{ \text{Weight loss at } T_2 \} - \{ \text{Weight loss at } T_1 \} \dots 5$$

Mechanical properties of QDC membrane

Tension tests of the QDC membrane were carried out using material testing system based on MTS Landmark 100/25, USA. The measurements were performed at a crosshead speed of 2 mm/min at 25 °C. The specimens were rectangles with the size of 20mm×8mm. Five specimens were tested. The thicknesses were about 50µm.

X-ray Diffraction

The X-ray diffraction patterns of cellulose and QDC were obtained using wide-angle X-ray diffraction (XRD) diffractometer within radiation $\lambda=1.54\text{\AA}$, voltage of 40 kV and filament current of 40 mA. Scattered radiation was detected in the range of $2\theta = 5\text{--}70^\circ$, at a scan rate of $2^\circ/\text{min}$.

Scanning Electron Microscopy

The morphology of QDC membrane surfaces and their cross-sections were examined via high-resolution scanning electron microscopy (SEM) (QUANTA FEG 250, ESEM, operated with an accelerating voltage of 200 V–30 kV and an operating voltage of 5–30 kV). The dried QDC membranes were previously coated with gold using S150A Sputter Coater-Edwards.

3. Results and discussion

Porosity, swelling, and water uptake

The effect of changing PEG content (0.0, 2.0, 5.0, 10.0, 15.0, 20.0 wt.% of the cellulose) on porosity, water uptake, and swelling of the QDC membranes was investigated. The results are presented in **Figure 2**. It is well known that PEG is a hydrophilic water-soluble polymer and, therefore, it aids in the formation of pores during the subsequent casting deposition step [37]. Consequently, PEG dissolves into the water phase during the coagulation process, leaving pores on the membrane matrix, which results in an increase in the membrane porosity and thus an increase in the surface area required for the adsorption process.

It is obvious from these data that increasing the PEG content leads to a rise in the porosity of QDC membrane from 11.7% (for the pristine) to reach 51.6% for QDC15. Consequently, both water uptake and swelling are significantly increased. This is attributed to the hydrophilic characteristics of the polar functional groups and their uniform desorption in QDC membranes [38]. The increase of PEG content resulted in increased porosity and, consequently, the enlargement of wet membrane

hydrophilicity. Therefore, this causes instantaneous phase de-mixing between solvent (acetone) and non-solvent (water) during membrane fabrication [39,40] which in turn increases the pores and voids within the membrane matrix. With a further increase in PEG content (20 wt.%), the porosity slightly decreased which may be due to the aggregation of such pore former during the de-mixing process. Therefore, up to 15 wt. % of PEG is considered the optimal pore former content for membrane fabrication.

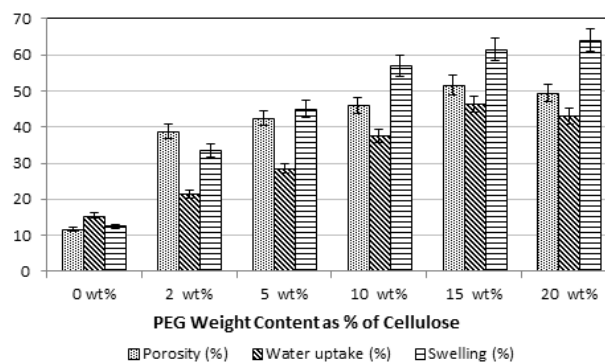


Figure 2: Effect of PEG wt.% on porosity, swelling, and water uptake. Error bars represent standard deviation of test observations.

Ion-exchange capacities (IECs)

The measure of ion-exchange capacity (IEC) allows for the determination of the concentration of available active sites in the QDC membrane on a weight basis. The IEC is an essential parameter of the ion exchange membrane and is related to the amount of exchangeable ionic within the membrane [41]. Generally, an increase in membrane IECs lead to better-performing membranes and also to greater membrane swelling in water [42]. The IEC change for the different membranes with different PEG content is presented in **Table 1**. The IEC of the QDC membrane increased from 0.8 to 2.4 mmol/g, and the pristine QDC exhibited an IEC of 0.8 mmol/g.

Table 1. IECs for the QDC Membrane

| Membrane | PEG%* | Ion-exchange capacities (IECs)(mmol/g) |
|----------|-------|----------------------------------------|
| QDC0 | 0.0 | 0.80 ± 0.1 |
| QDC2 | 2.0 | 1.10 ± 0.1 |
| QDC5 | 5.0 | 1.34 ± 0.1 |
| QDC10 | 10.0 | 1.94 ± 0.1 |
| QDC15 | 15.0 | 2.40 ± 0.1 |
| QDC20 | 20.0 | 2.28 ± 0.1 |

* PEG content as wt.% of cellulose

As expected, the water uptake and swelling increased with the increase in IEC. At high IEC values, water

absorption was relatively high, which may indicate that the amount of quaternary ammonium groups in the QDC membrane directly increases the water content. The IEC value of QDC20 was slightly lower than QDC15, which could be attributed to using PEG above the optimal content (15 wt. %) leading to agglomeration during membrane preparation. However, there is no significant statistical difference between IEC values of QDC 15 and QDC20. Overall, QDC15 provides the highest IEC value (2.4 mmol/g), and consequently, 15 wt.% of PEG seems to be the optimum amount of the pore former.

Thermal Stability of QDC

The thermal behavior of QDC and cellulose was analyzed using TGA, and the results are presented in **Figure 3**. In this figure, cellulose possessed a primary weight loss of around 270 °C, which was ascribed to the unstable hydroxyl groups removed from the main chain. The high weight loss from 350 °C can be attributed to the decomposition of the polymer main chain. For QDC, the first weight loss started at 215 °C, which was 55°C lower than the cellulose, suggesting that more unstable groups exist on the QDC, that is, quaternized dimethylamine groups. Note that both cellulose and QDC showed a slight weight loss below 100 °C because of the water evaporation.

The degree of substitution in QDC was calculated from the TGA curves [43]. T_1 represents the initial decomposition temperature of QDC, which is attributed to the decomposition of quaternary ammonium groups on the QDC surface. T_2 represents the initial decomposition temperature of cellulose, which is attributed to the decomposition of unstable hydroxyl in cellulose; this temperature can be regarded as the end point of quaternary ammonium groups decomposition approximately.

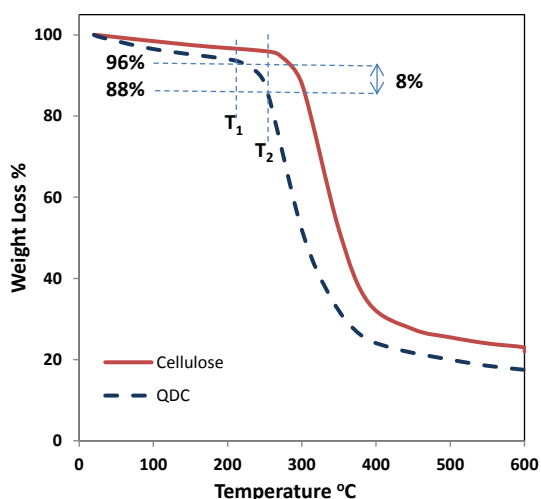


Figure 3: TGA curves of Cellulose and QDC

Therefore, the quaternary ammonium group content was calculated by the weight loss of QDC between T_1 and T_2 . As a result, the degree of substitution in QDC was found to be 8.0 wt%. We note the uncertainty associated with determining the degree of substitution is attributed to the challenge in determining the temperature of quaternary ammonium groups decomposition with high accuracy [44].

Mechanical properties of QDC membrane

The tensile strength of the QDC membrane with a different weight content of the pore former PEG is presented in **Figure 4**. Adding the PEG to synthesize the membrane decreased the tensile strength from 2.3 MPa for blank QDC membrane to reach 0.6 MPa for the membrane incorporating 20 wt.% PEG. The reduction in the tensile strength due to the increase in the membrane porosity is an anticipated result. The optimal QDC membrane with 15 wt.% content considered the optimal membrane showed a tensile strength of 1.2 MPa. This strength is sufficient to handle the membrane without damaging it.

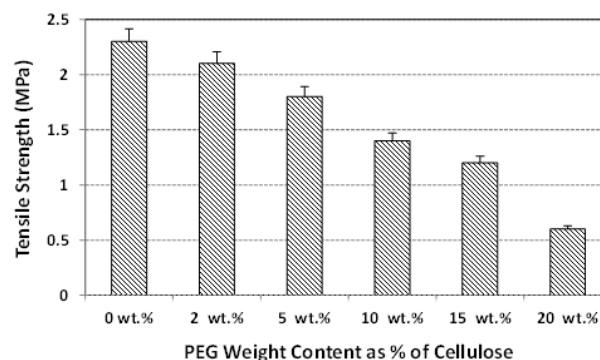


Figure 4: Tensile strength of QDC membrane. Error bars represent standard deviation of test observations.

Microstructural Analysis

X-ray Diffraction

The effect of functionalization of cellulose was examined with XRD technique. It is well known that cellulose material includes crystalline phase and amorphous phase[45]. Therefore, the crystallinity of cellulose and QDC were compared using XRD to study the effect of quaternization on the crystallinity of cellulose. The X-ray diffraction patterns of cellulose and QDC were shown in **Figure 5** and the crystallinity index (I_c) for each was calculated using Equation 6 [46]:

$$I_c = \frac{\{I_{(002)} - I_{(am)}\}}{I_{(002)}} \times 100 \dots \dots \dots 6$$

where $I_{(002)}$ is the counter reading at peak intensity of 2θ angle close to 22° representing crystalline phase and $I_{(am)}$ is the counter reading at peak intensity of 2θ angle close to 18° representing amorphous phase. It was found that the crystallinity index was 70.4% for cellulose and it was 49.8% for QDC. This is an

evident that attaching of quaternized ammonium group on the cellulose surface during the quaternization process; decreases the crystallinity of cellulose. However, the still remained crystalline phase in QDC indicates that quaternized cellulose (QDC) was generated without the destruction of cellulosic units.

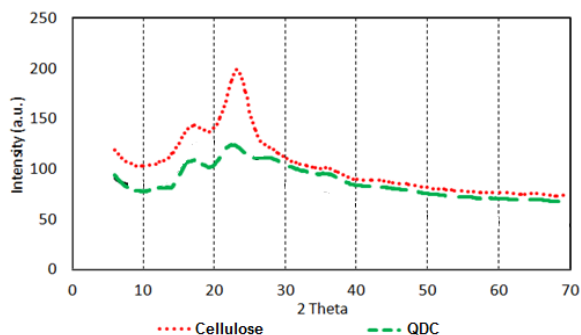
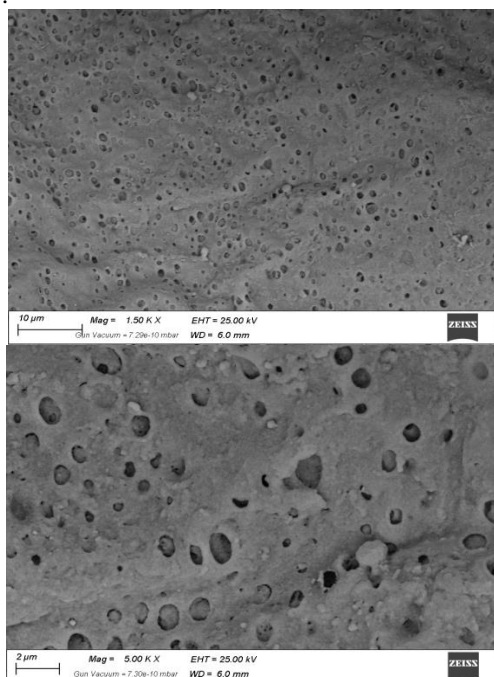


Figure 5: XRD for Cellulose and QDC

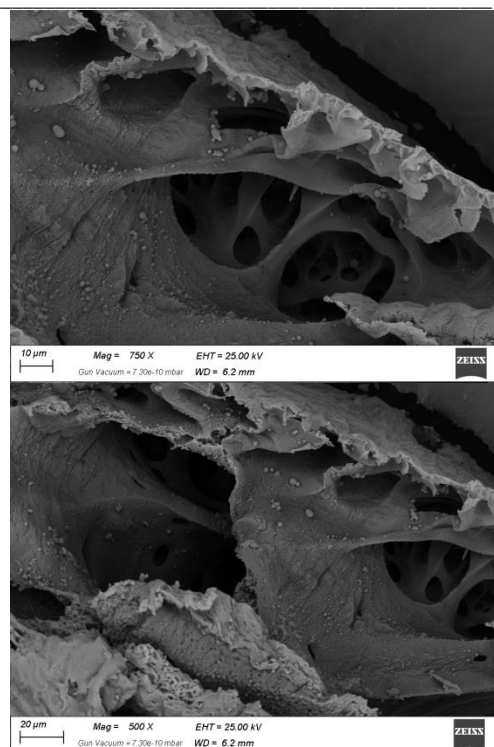
Scanning Electron Microscopy (SEM)

SEM analysis has been performed to investigate the main features of QDC membrane incorporating the optimal PEG content.

The QDC15 membrane surface morphology fabricated with the optimum content of the pore former (15 wt.% of PEG) was obtained at different magnifications, and the SEM results are shown in **Figure 6**. The surface of the membrane had small pores that were noted to be homogeneously distributed on the entire surface (**Figure 6a**). Moreover, the cross-section of the membrane appeared to be a multilayer with large pores (**Figure 6b**).



(a) Surface of QDC membrane



(b) Cross-section of QDC membrane

Figure 6: SEM analysis of (a) surface, & (b) cross-section of QDC15 membrane

This indicates a well-dissolved process during membrane preparation and the effective sonication step used for distributing the PEG into the cellulose phase during the fabrication process. In addition, these also indicate the spontaneous de-mixing during the immersion of the membrane solution in the coagulation bath (phase inversion technique) [47,48,49]. The large pores and macro-voids seem to enhance the interaction between the water phase and the ammonium groups on the QDC membrane and consequently enhanced the IEC value.

Fourier Transform Infrared Spectroscopy (FTIR)

The performed chemical modification for cellulose has been assured by comparing FTIR for cellulose, CDC QDC samples, as shown in **Figure 7**. In these FTIR spectra, cellulose shows a typical stretching peak for hydroxyl groups at $3200\text{--}3500\text{ cm}^{-1}$. Symmetric and asymmetric stretching peaks of CH, CH₂ and CH₃ appear at $2780\text{--}2980\text{ cm}^{-1}$. The OH bending vibrations of cellulose are located at 1630 cm^{-1} and C-O stretching vibration is observed at 1050 cm^{-1} . Bending vibration peaks of CH₂ and CH₃ appeared at 1390 cm^{-1} [50,51,52].

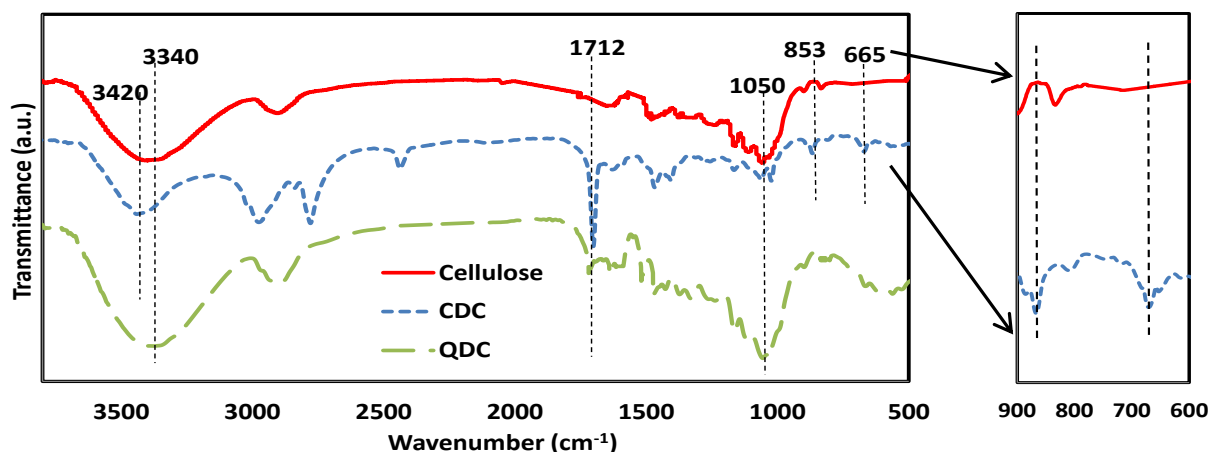


Figure 7: FTIR spectroscopy for cellulose, CDC and QDC

Comparing the FTIR spectra of cellulose, CDC and QDC exhibit some changes. The chlorination of cellulose is confirmed by the presence of two new peaks at 665 and 853 cm^{-1} which are attributed to C-Cl stretching frequency [53,54,55]. In addition, these peaks are significantly decreased in QDC, which indicates an effective quaternization reaction. The C=O stretching vibration (1712 cm^{-1}) peak that appeared on the sample indicated that some parts of un-substituted hydroxyl groups on CDC and QDC samples oxidized further into ketone groups [56,57]. In CDC, the O-H stretching vibration is shifted from 3340 cm^{-1} to 3420 cm^{-1} which is an indication of successful chlorination of cellulose. This shifting is due to the difference in the hydrogen bonding interaction of the hydroxyl groups in CDC and in cellulose [58,59]. The broad peak appearing over 3150-3550 cm^{-1} which is attributed to O-H stretching vibration of the QDC membrane, indicates successful alkalization of $\{\text{N}^+(\text{CH}_3)_3\text{Cl}^-\}$ groups into $\{\text{N}^+(\text{CH}_3)_3\text{OH}^-\}$ groups [60,61]. The broad peak of QDC has a stronger signal than that of cellulose.

Conclusion

A simple process to fabricate anion exchange membrane using inexpensive biomaterials (cellulose) is presented. The simple process incorporates functionalization of the cellulose, quaternization of the functionalized cellulose, polymer blending, and membrane fabrication. The membrane porosity was controlled by controlling the PEG pore former content. It was found that a PEG content of 15% by weight of the cellulose can produce optimal membrane characteristics. The porosity, water uptake, and swelling of the fabricated membranes were characterized. The ion-exchange capacities of the membranes were also measured. Furthermore, microstructural investigations of the membranes using SEM and FTIR were conducted. The investigation shows that fabricated QDC membranes with good ion-exchange capacities could be successfully fabricated.

Conflicts of interest

There are no conflicts to declare.

Acknowledgements

This research work was supported by Science, Technology & Innovation Funding Authority (STDF) under the grant (BARG Call7 - Project ID 37200). The authors greatly acknowledge this funding.

References

- [1] M.A.Eltawil, Z. Zhengming, L. Yuan, A review of renewable energy technologies integrated with desalination systems. *Renew. Sustain. Energy Rev.*, Vol. 13, pp (2245-2262), 2009.
- [2] Al-Mamun A., Baawain, M.S., Dhar, B., Kim, I.S., Improved recovery of bioenergy and freshwater in an osmotic microbial fuel cell using micro-diffuser assisted marine aerobic biofilm on cathode. *Biochem. Eng. J.* Vol. 128, pp (235-242), 2017.
- [3] M.F. Shaaban, M.A. El-Khateeb; M.A. Saad; Water Desalination Using Cellulosic Nano-filtration Membrane Composed of Nano-scale Polytetrafluoroethylene; *Egypt. J. Chem.* Vol. 62, No.1 pp.15 - 20 (2019)
- [4] W. Juda, W.A. McRae, Coherent ion-exchange gels and membranes. *J. Am. Chem. Soc.* 1950, 72, 1044. <https://doi.org/10.3390/ma9050365>
- [5] M.A. Abd El-Ghaffar, M.M. Elawady, A.M. Rabie, A.E. Abdelhamid, Enhancing the RO performance of cellulose acetate membrane using chitosan nanoparticles, *Journal of Polymer Research* (2020) 27:337, pp (1-12). <https://doi.org/10.1007/s10965-020-02319-7>
- [6] Tanaka, Yoshinobu (2015). *Ion exchange membranes: fundamentals and applications*. Japan: Elsevier. p. 47. ISBN 978-0-444-63319-4.
- [7] Strathmann, Heiner (2004). *Membrane Science and Technology Series, 9: Ion Exchange Membrane Separation Processes (First ed.)*. San

- Diego, Ca, USA: Elsevier. pp. 90–206. ISBN 0-444-50236-X.
- [8] Aly Al-Sayed, W.M. El-Senousy, A.Z. Al-Herrawy, M.M. Abo Aly, F.A. El-Gohary; Membrane Bioreactor Technology for Wastewater Reclamation; Egypt. J. Chem. Vol. 61, No.5 pp. 883 - 896 (2018)
- [9] Eman H. Abd Elnasser, Manara A. Ayoub#, Mona. A. Ahmed and Mariam G.R. ; Synthesis and Characterization of N-(2-acetylthiophene) salicylideneimine (ATS) as Ionophore for Polymeric Membrane Ag(I) Selective Electrode; Egypt. J. Chem. 59, No.6, pp.1001 –1012 (2016).
- [10] Hussein I. Abdel-Shafy, Sally H. Abdel-Shafy; Membrane Technology for Water and Wastewater Management and Application in Egypt; Egypt. J. Chem. Vol 60, No.3 pp. 347 - 360 (2017).
- [11] M.I. Khan, R. Luque, S. Akhtar, A. Shaheen, A. Mehmood, S. Idress, S.A. Buzdar, A. Rehman, Design of Anion Exchange Membranes and Electrodialysis Studies for Water Desalination. Materials, 9, 365, 2016. <https://doi.org/10.3390/ma9050365>
- [12] C.H. Zhao, Y. Gong, Q.L Liu, Q.G. Zhang, A.M. Zhu, Self-crosslinked anion exchange membranes by bromination of benzylmethyl-containing poly(sulfone)s for direct methanol fuel cells. Int. J. Hydrogen Energy, Vol. 37, pp (11383–11393), 2012.
- [13] J. Yan, M.A. Hickner, Anion exchange membranes by bromination of benzylmethyl-containing poly(sulfone)s. Macromolecules, Vol. 43, pp (2349–2356), 2010.
- [14] T. Xu, W. Yang, A novel positively charged composite membranes for nanofiltration prepared from poly(2,6-dimethyl-1,4-phenylene oxide) by in situ amines crosslinking. J. Membr. Sci., Vol. 215, pp (25–32), 2003.
- [15] Z. Lin, T. Xu, L. Zhang, Radiation-induced grafting of N-isopropylacrylamide onto the brominated poly(2,6-dimethyl-1,4-phenylene oxide) membranes. Radiat. Phys. Chem., Vol. 75, pp (532–540), 2006.
- [16] M.R. Hibbs, C.H. Fujimoto, C.J. Cornelius, Synthesis and characterization of poly(phenylene)-based anion exchange membranes for alkaline fuel cells. Macromolecules, Vol. 42, pp (8316–8321), 2009.
- [17] Z. Liu, X. Li, K. Shen, P. Feng, Y. Zhang, X. Xu, W. Hu, Z. Jiang, B. Liu, M.D. Guiver, Naphthalene-based poly(arylene ether ketone) anion exchange membranes. J. Mater. Chem. A, Vol. 1, pp (6481–6488), 2013.
- [18] U.S. Orlando, T. Okuda, A.U. Baes, W. Nishijima, M. Okada; Chemical properties of anion-exchangers prepared from waste natural materials; Reactive & Functional Polymers, Vol. 55, pp (311–318), 2003.
- [19] M A. Ahmed, M. El-Shafie, U F. Kandil, M. M. R Taha; Improving the Mechanical Properties of Thermoplastic Polyolefins Using Recycled Low-Density Polyethylene and Multi-Walled Carbon Nanotubes; Egyptian Journal of Chemistry, Vol. 64, No. 5, pp (2517-2523), 2021. <https://doi.org/10.21608/ejchem.2021.62554.3341>
- [20] E.C. Filho, J.C.P. de Melo, M.G. da Fonseca, C. Airoidi; Cation removal using cellulose chemically modified by a Schiff base procedure applying green principles; Journal of Colloid and Interface Science 340 (2009) 8–15.
- [21] U.S.Orland; T.OkudaA.U.BaesW.NishijimaM.Okada, Chemical properties of anion-exchangers prepared from waste natural materials; Reactive and Functional Polymers; Vol. 55, No. 3, , Pages 311-318; 2003
- [22] C. Zhang, J. Hu, W. Fan, M. K.H. Leung, Y. Meng; Plasma-grafted anion-exchange membrane preparation and process analysis; Electrochimica Acta 204 (2016) 218–226. <http://dx.doi.org/10.1016/j.electacta.2016.04.078>
- [23] Tatsuo Tashiro, Yukio Shimura, “Removal of Mercuric Ions by Systems Based on Cellulose Derivatives”; Journal of Applied Polymer Science, Vol. 27,747-756 (1982)
- [24] E.C. Filho, J.C.P. de Melo, M.G. da Fonseca, C. Airoidi; Cation removal using cellulose chemically modified by a Schiff base procedure applying green principles; Journal of Colloid and Interface Science 340 (2009) 8–15
- [25] U.S.Orland; T.OkudaA.U.BaesW.NishijimaM.Okada, Chemical properties of anion-exchangers prepared from waste natural materials; Reactive and Functional Polymers; Vol. 55, No. 3, , Pages 311-318; 2003
- [26] E.S. Mansor, A. Labena, R.M. Moghazy, A.E. Abdelhamid; Advanced eco-friendly and adsorptive membranes based on Sargassum; Journal of Water Process Engineering 37 (2020) 101424. <https://doi.org/10.1016/j.jwpe.2020.101424>
- [27] A.E. Abdelhamid, A.M. Khalil, Polymeric membranes based on cellulose acetate loaded with candle soot nanoparticles for water desalination, J. Macromol. Sci. Part A 0 (2019) 1–9, <https://doi.org/10.1080/10601325.2018.1559698>.
- [28] P. Moradihamedani, K. Kalantari, A.H. Abdullah, N.A. Morad, High efficient removal of lead(II) and nickel(II) from aqueous solution by novel polysulfone/Fe3O4–talc nanocomposite mixed matrix membrane, Desalin. Water Treat. 57

- (2016) 28900–28909, <https://doi.org/10.1080/19443994.2016.1193449>.
- [29] C. Zhang, J. Hu, W. Fan, M. K.H. Leung, Y. Meng; Plasma-grafted anion-exchange membrane preparation and process analysis; *Electrochimica Acta* 204 (2016) 218–226. <http://dx.doi.org/10.1016/j.electacta.2016.04.078>
- [30] X. Fan, Y. Su, X. Zhao, Y. Li, R. Zhang, Fabrication of polyvinyl chloride ultra filtration membranes with stable antifouling property by exploring the pore formation and surface modification capabilities of polyvinyl formal, *J. Memb. Sci.* 464: 100-109, (2014) – <https://doi.org/10.1016/j.memsci.2014.04.005>.
- [31] H. Rabiee, V. Vatanpour, M. Hossein, D. Abadi, H. Zarrabi, Improvement in flux and antifouling properties of PVC ultrafiltration membranes by incorporation of zinc oxide (ZnO) nanoparticles, *Sep. Purif. Technol.* 156:299–310,(2015). <https://doi.org/10.1016/j.seppur.2015.10.015>.
- [32] Y. Cao, K. Scott, X. Wang, Preparation of polytetrafluoroethylene porous membrane based composite alkaline exchange membrane with improved tensile strength and its fuel cell test, *International Journal of Hydrogen Energy*, Vol. 37, No. 17, pp (12688-12693) 2012. <https://doi.org/10.1016/j.ijhydene.2012.05.134>.
- [33] M.R. Mohamed, H.M. Naguib, R.A. El-Ghazawy, N.O. Shaker, A.A. Amer, A.M. Soliman, and U.F. Kandil, "Surface Activation of Wood Plastic Composites (WPC) for Enhanced Adhesion with Epoxy Coating", *Journal of Materials Performance and Characterization*, Vol 8, No. 1, pp (22–40), 2019. DOI: 10.1520/MPC20180034.
- [34] C. Zhang, J. Hu, W. Fan, M. K.H. Leung, Y. Meng; Plasma-grafted anion-exchange membrane preparation and process analysis; *Electrochimica Acta* 204 (2016) 218–226. <http://dx.doi.org/10.1016/j.electacta.2016.04.078>
- [35] C. Zhang, J. Hu, M. Nagatsu, Y. Meng, W. Shen, H. Toyoda, X. Shu, High-performance plasma-polymerized alkaline anion-exchange membranes for potential application in direct alcohol fuel cells, *Plasma Process. Polym.* 8 (2011) 1024–1032.
- [36] X. Cheng, J. Wang, Y. Liao, C. Li, Z. Wei; "Enhanced Conductivity of Anion-Exchange Membrane by Incorporation of Quaternized Cellulose Nanocrystal"; *ACS Appl. Mater. Interfaces*, Vol. 10, pp (23774–23782), **2018**. DOI: 10.1021/acsami.8b05298
- [37] A. Ahmad, S. Waheed, S.M. Khan, S. e-Gul, M. Shafiq, M. Farooq, K. Sanaullah, T. Jamil, Effect of silica on the properties of cellulose acetate/polyethylene glycol membranes for reverse osmosis, *Desalination* 355 (2015) 1–10, <https://doi.org/10.1016/j.desal.2014.10.004>.
- [38] L.T.T. Nhung, I.Y. Kim, Y.S. Yoon; Quaternized Chitosan-Based Anion Exchange Membrane Composited with Quaternized Poly(vinylbenzyl chloride)/Polysulfone Blend; *Polymers* 2020, 12, 2714; doi:10.3390/polym12112714.
- [39] E.S. Mansor, A. Labena, R.M. Moghazy, A.E. Abdelhamid; Advanced eco-friendly and adsorptive membranes based on Sargassum; *Journal of Water Process Engineering* 37 (2020) 101424. <https://doi.org/10.1016/j.jwpe.2020.101424>
- [40] P. Moradihamedani, N.A. Ibrahim, D. Ramimoghadam, W.M.Z.W. Yunus, N.A. Yusof, Polysulfone/zinc oxide nanoparticle mixed matrix membranes for CO₂/CH₄ separation, *J. Appl. Polym. Sci.* 131 (2014) 1–9, <https://doi.org/10.1002/app.39745>.
- [41] L.T.T. Nhung, I.Y. Kim, Y.S. Yoon; Quaternized Chitosan-Based Anion Exchange Membrane Composited with Quaternized Poly(vinylbenzyl chloride)/Polysulfone Blend; *Polymers* 2020, 12, 2714; doi:10.3390/polym12112714.
- [42] S.M. MacKinnon, T.J. Fuller, F.D. Coms, M.R. Schoeneweiss, C.S. Gittleman, Y.-H. Lai, R. Jiang, A.M. Brenner, FUEL CELLS – PROTON-EXCHANGE MEMBRANE FUEL CELLS | Membranes: Design and Characterization, *Encyclopedia of Electrochemical Power Sources*, pp (741-754), 2009. <https://doi.org/10.1016/B978-044452745-5.00905-9>.
- [43] X. Cheng, J. Wang, Y. Liao, C. Li, Z. Wei; "Enhanced Conductivity of Anion-Exchange Membrane by Incorporation of Quaternized Cellulose Nanocrystal"; *ACS Appl. Mater. Interfaces*, Vol. 10, pp (23774–23782), **2018**. DOI: 10.1021/acsami.8b05298
- [44] X. Cheng, J. Wang, Y. Liao, C. Li, Z. Wei; "Enhanced Conductivity of Anion-Exchange Membrane by Incorporation of Quaternized Cellulose Nanocrystal"; *ACS Appl. Mater. Interfaces*, Vol. 10, pp (23774–23782), **2018**. DOI: 10.1021/acsami.8b05298
- [45] Na Ma, Dongyan Liu, Yueyue Liu, Guoxin Sui. Extraction and Characterization of Nanocellulose from Xanthoceras Sorbifolia Husks. *International Journal of Nanoscience and Nanoengineering*. Vol. 2, No. 6, pp(43-50), 2015.
- [46] Mwaikambo LY, Ansell MP. Chemical modification of hemp, sisal, jute, and kapok fibers by alkalization. *J Appl Polym Sci*; Vol. 84, pp(2222-2234), 2002.
- [47] A. Labena, A.E. Abdelhamid, A.S. Amin, S. Husien, L. Hamid, G. Safwat, A. Diab, A. A.

- Gobouri, E. Azab; Removal of Methylene Blue and Congo Red Using Adsorptive Membrane Impregnated with Dried *Ulva fasciata* and *Sargassum dentifolium*; *Plants* 2021, 10, 384. <https://doi.org/10.3390/plants10020384>.
- [48] A.E.Abdelhamid; A.A.El-Sayed; A.M. Khalil, Polysulfone nanofiltration membranes enriched with functionalized grapheme oxide for dye removal from wastewater. *J. Polym. Eng.* 2020, 40, 833–841.
- [49] S.H. Khan; B.Pathak, Zinc oxide based photocatalytic degradation of persistent pesticides: A comprehensive review. *Environ. Nanotechnol. Monit. Manag.* 2020, 13, 100290.
- [50] I. Kim, J. Kim, D. Lee; Sulfonic acid functionalized deoxycellulose catalysts for glycerolacetylation to fuel additives; *Applied Catalysis A: General* 482 (2014) 31–37
- [51] D.L. Pavia, G.M. Bassler, T.C. Morrill, *Introduction to Spectroscopy*, second ed., Saunders College Publishing, New York, 1996.
- [52] G.R. Castro, I.L. Alcântara, P.S. Roldan, D.F. Bozano, P.M. Padilha, A.O. Florentino, J.C. Rocha, *Mater. Res.* 7 (2004) 329.
- [53] Silverstein, R.M., Basler, G.C., Morrill, T.C., “Traduction de la cinquieme edition de «Spectrometric Identification of Organic Compound»”, Wiley, 124-130 (1991).
- [54] <https://www.sigmaaldrich.com/technical-documents/articles/biology/ir-spectrum-table.html>
- [55] <https://orgchemboulder.com/Spectroscopy/irtutor/alkhalidesir.shtml>
- [56] I. Kim, J. Kim, D. Lee; Sulfonic acid functionalized deoxycellulose catalysts for glycerolacetylation to fuel additives; *Applied Catalysis A: General* 482 (2014) 31–37
- [57] S.H. Zeronian, M.K. Inglesby, *Cellulose* 2 (1995) 265–272.
- [58] M. Emiroglu, A.E. Douba, R.A. Tarefder, , U.F. Kandil, M.M. Reda Taha, “New Polymer Concrete with Superior Ductility and Fracture Toughness Using Alumina Nanoparticles”; *Journal of Materials in Civil Engineering*; Vol. 29, No. 8, 04017069, 2017. [https://doi.org/10.1061/\(ASCE\)MT.1943-5533.0001894](https://doi.org/10.1061/(ASCE)MT.1943-5533.0001894)
- [59] Y. Mikhaylova, G. Adam, L. Häussler, K. J. Eichhorn, and B. Voit. (2006). “Temperature-dependent FTIR spectroscopic and thermoanalytic studies of hydrogen bonding of hydroxyl (phenolic group) terminated hyperbranched aromatic polyesters.” *J. Molecular Struct.*, 788(1–3), 80–88.
- [60] C. Zhang, J. Hu, W. Fan, M. K.H. Leung, Y. Meng; Plasma-grafted anion-exchange membrane preparation and process analysis; *Electrochimica Acta* 204 (2016) 218–226. <http://dx.doi.org/10.1016/j.electacta.2016.04.078>
- [61] A. Asadinezhad, I. Novak, M. Lehocky, V. Sedlarik, A. Vesel, I. Junkar, P. Saha, I. Chodak, A physicochemical approach to render antibacterial surfaces on plasma-treated medical-grade PVC: irgasan coating, *Plasma Process. Polym.* 7 (2010) 504–514.